J. Cent. South Univ. (2014) 21: 1907−1918
DOI: 10.1007/s11771-014-2137-7

Springer

Fast image matching algorithm based on affine invariants

ZHANG Yi(张毅)[1, 2], LU Kai(卢凯)[1, 2], GAO Ying-hui(高颖慧)[3]

1. National Laboratory for Parallel and Distributed Processing (National University of Defense Technology), Changsha 410073, China;
2. College of Computer, National University of Defense Technology, Changsha 410073, China;
3. College of Electronic Science and Engineering, National University of Defense Technology, Changsha 410073, China

Abstract: Feature-based image matching algorithms play an indispensable role in automatic target recognition (ATR). In this work, a fast image matching algorithm (FIMA) is proposed which utilizes the geometry feature of extended centroid (EC) to build affine invariants. Based on affine invariants of the length ratio of two parallel line segments, FIMA overcomes the invalidation problem of the state-of-the-art algorithms based on affine geometry features, and increases the feature diversity of different targets, thus reducing misjudgment rate during recognizing targets. However, it is found that FIMA suffers from the parallelogram contour problem and the coincidence invalidation. An advanced FIMA is designed to cope with these problems. Experiments prove that the proposed algorithms have better robustness for Gaussian noise, gray-scale change, contrast change, illumination and small three-dimensional rotation. Compared with the latest fast image matching algorithms based on geometry features, FIMA reaches the speedup of approximate 1.75 times. Thus, FIMA would be more suitable for actual ATR applications.

Key words: affine invariants; image matching; extended centroid; robustness; performance

1 Introduction

Image matching is utilized in digital image processing for recognizing the target in an image by automatically matching a template image from the database of target patterns. It is widely used in computer vision, medical imaging, website image retrieval, military automatic target recognition, and optical image analyzing. Because there may exist affine transformations (shift, rotation, zoom and shape deformation), partial occlusion and different surroundings between samplings of the same object, image matching is difficult to recognize targets correctly. In Fig. 1, some actual example images of Mac logo in the Internet are shown, and recognizing the logo from different images correctly and automatically will be a challenge task. Therefore, the construction of building accurate target recognition algorithms based on image matching has been extensively investigated in the past decades.

There are two categories of image matching algorithms [1]: the template-based and the feature-based. The former ones recognize targets through the comparison

Fig. 1 Examples of Mac Logo in some web images

of the gray-scale diversity between the reference and observed images. It could work well for the image with small size and small gray-scale range without complex pre-processing, yet it is invalid when changing the viewpoint of sensors or the gray-scale range. Hence, it is not suitable for actual target recognition. Compared with the template-based algorithms, the feature-based ones utilize some invariable features to recognize targets and

Foundation item: Projects(2012AA010901, 2012AA01A301) supported by National High Technology Research and Development Program of China; Projects(61272142, 61103082, 61003075, 61170261, 61103193) supported by the National Natural Science Foundation of China; Projects(B120601, CX2012A002) supported by Fund Sponsor Project of Excellent Postgraduate Student of NUDT, China
Received date: 2012−12−11; **Accepted date:** 2013−07−10
Corresponding author: LU Kai, Professor; Tel: +86−13407316868; E-mail: kailu@nudt.edu.cn

have better robustness for the change of viewpoint. However, it is found that the development of the image matching algorithms based on features has been limited by the weak robustness for disturbance, the invalidation problem during extracting features and the low computing performance [2−3].

In this work, in order to recognize the single target in an optical image accurately, a fast image matching algorithm (FIMA) is designed which utilizes global geometry feature to build affine invariants. FIMA is based on affine invariant feature of the length ratio of two parallel line segments. Hence, it addresses the invalidation problem of the state-of-the-art algorithms based on affine geometry, and increases the feature diversity of different targets to reduce misjudgment rate during recognizing targets. Moreover, AD-FIMA, an advanced FIMA, is designed to overcome two disadvantages of FIMA. Simulation results illustrate the performance enhancement and better robustness for noise, gray-scale change, contrast change, illumination as well as small three-dimensional rotation of the proposed algorithms compared with the existing algorithms. In Fig. 2, two examples are shown to illustrate how to extract affine invariants features and matching images in our new algorithms.

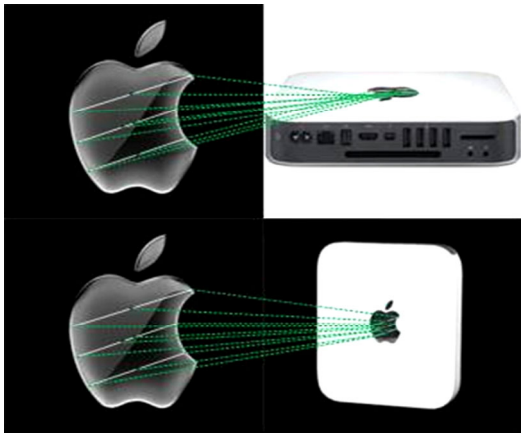

Fig. 2 Two examples of proposed algorithm

2 Related works

Many feature-based image matching algorithms have been explored, which include two categories: local feature-based and global feature-based [4]. Local feature-based algorithms (e.g. SIFT [5], SURF [6], MSER [7] and RASIM [8]) focus on multiple interest points by computing some properties of the local image neighborhoods. One advantage of using local features is that they could be used to recognize targets even if significant clutter and occlusion exist. However, when the target is single or quite accurate classifying is needed, the global feature-based algorithms are more suitable, because they utilize more information of the whole image and are more sensitive to some slight changes.

Recently, many global features have been extracted as the feature invariants of images, including computation features [2, 9] and geometry features [3, 10−13]. HU [2] found that the moments as a general computation feature of the image could be utilized to recognize targets, because the value ratios of different moments were maintained after affine transformation. However, its low performance and weak robustness for noise were pointed out [14]. RATHU et al [9] designed an algorithm based on multi-scale auto-convolution (MSA). MSA built affine feature invariants using the affine-invariable linear relation of random four points (it should be ensured that these four points are not in the same line) in the image. MSA has good robustness for noise, and it could work well even if partial occlusion and 3D transformation exist. However, the performance and robustness for gray-scale change of MSA are very weak.

Recently, the increasing algorithms based on geometry features have been exploited. CHRISTO et al [12] proposed to build affine invariants through extracting the contour feature of target. YANG and COHEN [13] utilized convex hull of some edge points to build several triangles, and designed affine invariants of the size ratios of triangles. But both of these two algorithms need the precise image segmentation and edge extraction. CHEN et al [10] proposed EC-ARC algorithm for the first time which utilized affine invariable extended centroid (EC) to build affine triangles for target recognition. EC-ARC does not depend on image segmentation and has good performance. However, when building affine triangles, some invalidation problem will happen because some ECs may be too near or in the same line so that the size of triangles may be approximately zero. LEI et al [3] and GAO and WEN [11] improved EC-ARC. LEI et al [3] combined EC-ARC with convex hull to build triangles. GAO and WEN [11] used affine quadrangles to replace triangles to recognize target. However, these improvements do not resolve the invalidation problem ultimately because they all still utilize the area size ratio to build affine invariants. Meanwhile, it is found that these affine areas based algorithms have much misjudgment rate during recognizing targets.

Owing to the aforementioned problems of the current image matching algorithms based on features, the three factors, namely how to design robust affine invariable features, how to resolve the invalidation problem of extracting features and how to enhance performance become the largest limitations for the development of the image matching algorithms based on features. In this work, FIMA, a fast image matching algorithm, will be designed to address these problems.

3 Fundamental theory

3.1 Affine invariant theory

If the depth of object is small enough compared with the distance between object and sensor, a general definition of affine transformation which shows the transformation between two different viewpoints for the same object can be expressed as [13]

$$\begin{bmatrix} X' \\ Y' \end{bmatrix} = \begin{bmatrix} a_{11} & a_{12} \\ a_{21} & a_{22} \end{bmatrix} \begin{bmatrix} X \\ Y \end{bmatrix} + \begin{bmatrix} b_1 \\ b_2 \end{bmatrix} \tag{1}$$

where $[X \quad Y]^{\mathrm{T}}$ and $[X' \quad Y']^{\mathrm{T}}$ denote the coordinates of a certain pixel before and after affine transformation, respectively. Let the parameters of affine transformation be denoted as $\boldsymbol{A} = \begin{bmatrix} a_{11} & a_{12} \\ a_{21} & a_{22} \end{bmatrix}$ and $\boldsymbol{B} = \begin{bmatrix} b_1 \\ b_2 \end{bmatrix}$. In general, $\det(\boldsymbol{A}) \neq 0$, if it is the transformation of two-dimensional image. This kind of affine transformation includes shift, rotation, zoom and shape deformation from the different viewpoints of an image.

From the definition, the four following theories could be proved [13].

Theorem 1: A line will still be a line after affine transformation.

Theorem 2: Two parallel lines will still be parallel after affine transformation.

Theorem 3: The linear relationship of three points in the same line will be maintained after affine transformation.

Theorem 4: The area ratio of any triangle before and after affine transformation will be a constant $|\det(\boldsymbol{A})|$. Moreover, the size ratio of any geometry regions before and after affine transformation will be also the constant $|\det(\boldsymbol{A})|$.

The algorithms of YANG and COHEN [13], EC-ARC [10], and GAO and WEN [11] are all based on Theorem 4, which is just the main reason of the invalidation problem. Consequently, this motivates us to find other theories to build affine invariants.

Lemma: The length ratio of two parallel line segments will be maintained after affine transformation.

Proof: Suppose AB and CD are two parallel line segments in an original image, i.e. $AB//CD$. In the image after affine transformation, they become $A'B'$ and $C'D'$. The example is shown in Fig. 3.

Apply **Theorem 2** and $AB//CD$, so $A'B'//C'D'$.

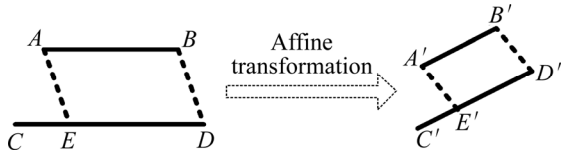

Fig. 3 Example of proof of Lemma

In the original image, connect BD and make an assistant line AE from A, where $AE//BD$ and E are the intersection of AE and CD. It is obvious that $d(AB)=d(ED)$, where $d()$ means the length of a line segment.

In the image after affine transformation, connect $B'D'$ and make an assistant line $A'E'$ from A', where $A'E'//B'D'$ and E' is the intersection of $A'E'$ and $C'D'$. Similarly, $d(A'B')=d(E'D')$.

Since A', B' and D' are the affine points of A, B and D, respectively, the parallelogram $A'B'D'E'$ is the affine area of the parallelogram $ABDE$. Hence, E' is also the affine point of E.

Therefore, $\dfrac{d(ED)}{d(CD)} = \dfrac{d(E'D')}{d(C'D')}$ can be known by applying Theorem 3. Subsequently, $\dfrac{d(AB)}{d(CD)} = \dfrac{d(A'B')}{d(C'D')}$ is proved.

In order to solve the invalidation problem mentioned in Section 2, Lemma will be utilized as the fundamental theory of our new algorithms to build affine invariants.

3.2 Extended centroid

According to the Lemma in Section 3.1, a new way is proved to build affine invariants. In order to find parallel line segments, we need to extract some feature points from the image firstly. In this work, the extended centroids (EC) is utilized which are global geometry feature points introduced in EC-ARC [10] and work by GAO and WEN [11].

In an image, a centroid is the pixel with the coordinate of (P_x, P_y):

$$\begin{cases} P_x = \dfrac{\iint_R xf(x,y)\mathrm{d}x\mathrm{d}y}{\iint_R f(x,y)\mathrm{d}x\mathrm{d}y} \\ P_y = \dfrac{\iint_R yf(x,y)\mathrm{d}x\mathrm{d}y}{\iint_R f(x,y)\mathrm{d}x\mathrm{d}y} \end{cases} \tag{2}$$

where $f(x, y)$ is the gray-scale of the pixel (x, y) in an image. R denotes the target region. Since the gray-scale of every point will be maintained after affine transformation, the affine point of the centroid will also be the centroid of the image after affine transformation [10].

Assume that $F(x, y)$ is a polynomial function of $f(x, y)$:

$$F(x,y) = af(x,y)^b, a \in \mathbf{R}, b \in \mathbf{Z} \tag{3}$$

According to Eq. (3), we could extract a pixel of which the coordinate is (P'_x, P'_y) in Eq. (4). It is the b-level EC of the target. It is apparent that when $n=a=b=1$, EC is the centroid. Therefore, it is considered that centroid is special EC.

$$\begin{cases} P'_x = \dfrac{\iint_R xF(x,y)\mathrm{d}x\mathrm{d}y}{\iint_R F(x,y)\mathrm{d}x\mathrm{d}y} \\ P'_y = \dfrac{\iint_R yF(x,y)\mathrm{d}x\mathrm{d}y}{\iint_R F(x,y)\mathrm{d}x\mathrm{d}y} \end{cases} \tag{4}$$

By comparing Eq.(4) with Eq.(2), it is easy to prove that the affine point of EC will also be the extended centroid of the image after affine transformation.

4 Fast image matching algorithm

In this section, the fast image matching algorithm FIMA is introduced in detail. Firstly, the workflow of FIMA to show how to recognize targets will be described. Next, by analyzing asymptotic complexities of some global feature-based algorithms and FIMA, it is manifested that FIMA outperforms the other algorithms. Then, the shortcomings of FIMA are discussed and AD-FIMA is designed to overcome these drawbacks.

4.1 Workflow of FIMA

To build affine invariants, FIMA utilizes some global geometry feature points ECs according to the Lemma in Section 3.1 along with the definition of EC to construct several pairs of parallel line segments in the image. By comparing the similarity of affine invariants between the reference and observed images, FIMA would give the decision of the category of target.

The detailed workflow of FIMA is shown as follows and an example is illustrated in Fig. 4.

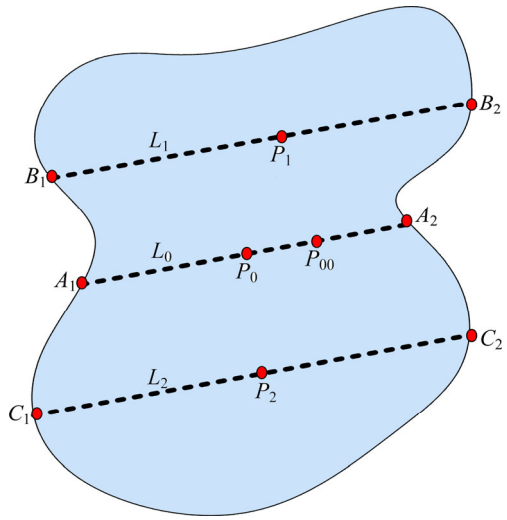

Fig. 4 Example of workflow of FIMA

Step 1: Utilize Eq. (2) to extract the centroid pixel P_0.

Step 2: Utilize Eq. (4) to extract the α-level extended centroid P_{00}.

Step 3: Make a line L_0 cross P_0 and P_{00}. Assume A_1 and A_2 are the two intersections between L_0 and the contour of target. Meanwhile, this image is divided into two sub-images by L_0.

Step 4: Utilize Eq. (2) again to extract the sub-centroid points of the two sub-images, and express them as P_1 and P_2, respectively.

Step 5: Make line L_1 cross P_1 and make sure $L_1//L_0$. Assume B_1 and B_2 are the two intersections between L_1 and the contour of the target. Meanwhile, in the other part symmetrically, make line L_2 cross P_2 and make sure $L_2//L_0$. Assume C_1 and C_2 are the two cross points between L_2 and the contour of the target.

Step 6: After Steps 1−5, some feature points and pairs of parallel line segments are constructed. Then build the affine invariants vector $\boldsymbol{F}$:

$$\begin{cases} \boldsymbol{F} = [\delta_i],\ i = 1,2,\cdots,6 \\ \delta_1 = \dfrac{d(A_1P_0)}{d(A_1A_2)},\ \delta_2 = \dfrac{d(A_1P_{00})}{d(A_1A_2)},\ \delta_3 = \dfrac{d(B_1P_1)}{d(B_1B_2)} \\ \delta_4 = \dfrac{d(C_1P_2)}{d(C_2C_2)},\ \delta_5 = \dfrac{d(A_1A_2)}{d(B_1B_2)},\ \delta_6 = \dfrac{d(A_1A_2)}{d(C_1C_2)} \end{cases} \tag{5}$$

It is apparently found that every δ_i is linearly independent.

Step 7: Calculate the diversity S of the reference and observed images in Eq. (6). The similarity of them is higher if S is smaller. According to the value of S, whether the target in observed image is the reference one would be known:

$$S = D(\boldsymbol{F},\boldsymbol{F}') = \frac{\|\boldsymbol{F}-\boldsymbol{F}'\|}{\|\boldsymbol{F}\|} = \sqrt{\frac{\sum_{i=1}^{6}(\delta_i-\delta'_i)^2}{\sum_{i=1}^{6}\delta_i^2}} \tag{6}$$

4.2 Asymptotic complexity

Performance is an important measurement to assess the availability of the image matching algorithms. Through analyzing several algorithms including HU [2], MSA [9], EC-ARC [10] and GAO and WEN [11], it is known that when processing a gray-scale image with size of $N\times N$, the time consumption of them are $O(N^2\log_2 N)$, $O(N^2)$, $2\alpha kN^2$ and $(2\alpha+K)N^2$, respectively, where α represents the level of EC, and K represents the number of centroids which need to search.

Then the asymptotic complexity of FIMA will be analyzed. In Ref. [11], it is reported that when utilizing centroids and ECs to build affine invariants, the main consumption of algorithm is extracting these feature points. In an image with size of $N\times N$, it will cost $2\alpha N^2$ to extract a α-level EC and N^2 to find a centroid or sub-centroid. In Section 4.1, FIMA needs to search three centroids and one extended centroid. Therefore, the complexity of FIMA is $(2\alpha+3)N^2$.

GAO and WEN's algorithm [11] is the fastest one in all the mentioned algorithms. To alleviate the invalidation problem, in the experiment, 9-level EC and 12 centroids are used, thus the algorithm costs approximately $30N^2$ to build an affine invariants vector with four parameters. Since the theory of FIMA avoids the computing of size of area, FIMA just needs to search a low-level EC (we use two-level EC in the experiment in Section 5) for most images, that is to say, it will cost totally $7N^2$ to build an affine invariants vector with six parameters. Therefore, it is qualitatively proved that FIMA has better performance and availability.

4.3 Advanced FIMA

In this section, some drawbacks of our proposed algorithm FIMA are pointed out and the advanced FIMA (AD-FIMA) is designed to enhance the basic method. Firstly, compared with FIMA, AD-FIMA could describe the diversity of different objects more precisely, especially for the objects with parallelogram contour, because it changes Step 6 in the workflow of FIMA. Secondly, through analyzing the different kinds of the invalidation problems in EC-ARC, an algorithm of extracting EC is utilized dynamically, and thus the difficulty of the coincidence between centroid and EC could be addressed.

4.3.1 Parallelogram contour

It is found that when the contour shape of target is parallelogram, more misjudgment rate happens during FIMA recognizing target. The reason is that all the parallel cut line segments have the same length in a parallelogram. As shown in Fig. 5, when extracting affine invariants features of the reference and observed images in Step 6 in Section 4.1, it appears that $\delta_5=\delta_6=1$ even if the objects of the two images are different but both parallelograms.

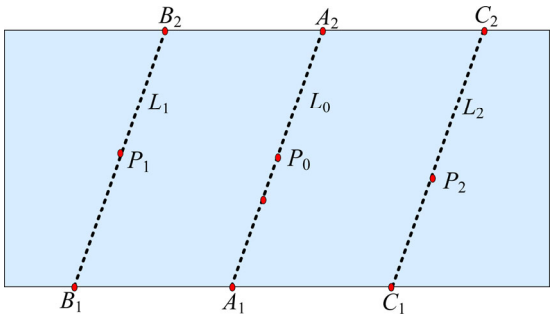

Fig. 5 Example of target with parallelogram contour

To address this problem, Step 6 of FIMA should be changed to build affine invariants. In the advanced FIMA (AD-FIMA), the length ratios of line segment pairs which do not depend on the contour are used to replace FIMA to recognize category of parallelogram target. In AD-FIMA, δ_5 and δ_6 are given as

$$\begin{cases}\delta_5=\dfrac{d(A_1P_0)}{d(B_1P_1)}\\ \delta_6=\dfrac{d(A_1P_0)}{d(C_1P_2)}\end{cases} \tag{7}$$

4.3.2 Coincidence of centroid and extended centroid

By avoiding utilizing the size ratio of affine areas, FIMA reduces the invalidation problem sharply, compared with EC-ARC and GAO. Yet, it is found that there still exist a few invalidation problems when extracting affine invariant features.

Through analyzing and rechecking these three algorithms, it is found that there are two categories of invalidation problems: the zero-feature invalidation and the coincidence invalidation. The former one means that the extracted geometry feature will be approximately zero, e.g. the size of some affine area. And it is the main reason of the invalidation problem. The later one is that the pixels of centroid and EC may be coincided in some certain probability. Because FIMA addresses the zero-feature invalidation, we now focus on the coincidence invalidation in FIMA.

By comparing Eq. (2) with Eq. (4), if the coincidence of the centroid (P_x,P_y) and the extended centroid (P'_x, P'_y) happens, $P_x=P'_x$ and $P_y=P'_y$. For the symmetry of the two dimensions, we just analyze $P_x=P'_x$ as example. It is shown as

$$\frac{\iint_R xf(x,y)\mathrm{d}x\mathrm{d}y}{\iint_R f(x,y)\mathrm{d}x\mathrm{d}y}=\frac{\iint_R xF(x,y)\mathrm{d}x\mathrm{d}y}{\iint_R F(x,y)\mathrm{d}x\mathrm{d}y} \tag{8}$$

This equals

$$\iint_R xf(x,y)\mathrm{d}x\mathrm{d}y*\iint_R F(x,y)\mathrm{d}x\mathrm{d}y=\iint_R f(x,y)\mathrm{d}x\mathrm{d}y*\iint_R xF(x,y)\mathrm{d}x\mathrm{d}y \tag{9}$$

In Eq. (9), because $f(x, y)$ and $F(x, y)$ are discrete and random as the diversity of different optical image, there exists small probability of the coincidence invalidation.

Meanwhile, for digital image, the error of image quantization [20−21] may also cause the coincidence invalidation when the centroid and EC are quite near. As shown in Eq. (10), when the two computing points make all true statements when being substituted into the three in equations, the two points may be quantized to the same pixel:

$$\begin{cases}\sqrt{(P'x-Px)^2}<1\\ \sqrt{(P'y-Py)^2}<1\\ \sqrt{(P'x-Px)^2+(P'y-Py)^2}<\sqrt{2}\end{cases} \tag{10}$$

We test all the 7200 images in COIL-100 database [10] and find the existence of the coincidence

invalidation changes as the level of EC. Figure 6 shows the relationship of the level of EC and the number of image where the coincidence invalidation exists.

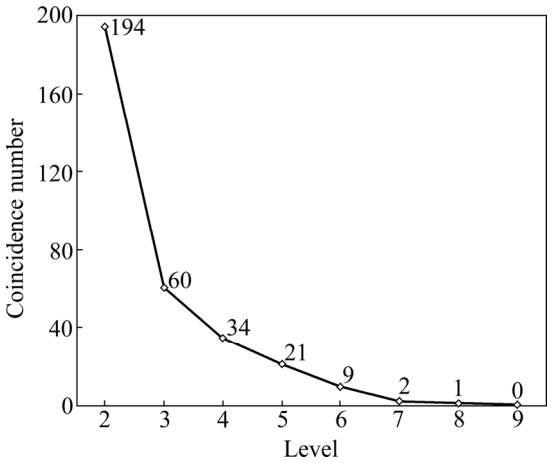

Fig. 6 Relationship of level of EC and number of images existing coincidence invalidation in COIL-100 database

In Fig. 6, when the two-level centroid is chosen to be EC, the coincidence invalidations happen in 194 images. With the rise of the level, the coincidence invalidation decreases sharply. When nine-level EC is chosen, no coincidence invalidations happen in all images in COIL-100.

In AD-FIMA, an algorithm of extracting EC dynamically is proposed to address the coincidence invalidation, according to the following two reasons. Firstly, because a fixed level EC is utilized in EC-ARC, GAO and FIMA, there exists the coincidence invalidation in all of them. Even if a higher-level EC is chosen, it does not ensure the probability of coincidence between centroids and the fixed EC is 0 for any actual image. Secondly, the time consumption of extracting a higher-level EC is much higher than a lower one.

The pseudo code of the algorithm of dynamically extracting EC is shown as follows:

```
Algorithm Extracting_EC
int L = 1; Pixel C is centroid;
while(L++){
Pixel EC is L-level extended centroid;
if (C and EC are coinciding)
   continue;
else
   break;
}EC is the extracted extended centroid.
```

In this algorithm, two variables are set: EC and L represent the final choice of EC and the level of EC, respectively. Beginning with 2-level EC, the whole procedure will try to find the minimum level EC which does not coincide with the centroid.

AD-FIMA could not only inherit the advantage of avoiding the zero-feature invalidation, but also address the coincidence invalidation by utilizing the algorithm of extracting EC dynamically. Therefore, AD-FIMA would never suffer from the invalidation problems when extracting the affine invariant features.

5 Experiment

In this section, the robustness and performance of FIMA and AD-FIMA will be assessed through some experiments. Comparisons are made between the two proposed algorithms and EC-ARC [10] and GAO and WEN [11]. All the four algorithms and the test procedures are coded in C language and run in the processor of Intel Core2 Quad CPU Q6600.

Image data of experiments are from COIL-100 [15]. In this database, there are totally 100 kinds of objects, and every object has 72 optical images with black background which are sampled from different viewpoints. Size of every original image is 128 pixel×128 pixel.

In our experiments, the five-level extended centroid is chosen to be the fixed EC in EC-ARC, GAO and FIMA. Meanwhile, because the parameter numbers of affine invariant vectors in EC-ARC and GAO are 5 and 4 respectively, in order to utilize Eq. (6) to calculate the diversity, all the vectors are assumed to have 6 parameters and the last one in EC-ARC and the last two in GAO will be assigned to be zero when extracting features.

Meanwhile, it is known that the contours extracting is an important pre-procedure of image matching. In this work, in order to extract the contours of targets, a fast and precise edge detector, R-SUSAN [16], is utilized which was designed by our group before.

5.1 Invalidation problem

Firstly, we focus on the invalidation problems of the four algorithms. Figure 7 depicts the average invalidation probability of the four algorithms when extracting the affine invariant features of all the objects. It is shown that the average invalidation probability of EC-ARC is about 12.6%. GAO makes a sharp improvement, which reduces the average probability to 1.15%. FIMA addresses the zero-feature invalidation, yet there exists some invalidation problem when extracting features in some certain images. However, the average probability of FIMA is 0.05% because of the coincidence invalidation. Through utilizing the algorithm of extracting EC dynamically, AD-FIMA enhances FIMA and never suffers from the invalidation problems when extracting the affine invariant features.

5.2 Diversity of different objects

Figure 8 demonstrates the average feature diversity between every object and others when applying these

four algorithms. It is found that the average diversity coefficients of EC-ARC and GAO are very small, which are 0.127 and 0.312, respectively. It is the main factor of the serious misjudgment rates of the two algorithms. Compared with them, FIMA and AD-FIMA could express the diversity of different objects more precisely. The average diversity of FIMA is 1.702. Since AD-FIMA addresses the parallelogram contour problems, it shows more precise features of targets and the average diversity is approximately 2.47. Thus, FIMA and AD-FIMA are more suitable to classify objects.

5.3 Robustness test

In order to test the robustness of these algorithms, some disturbances (additive white Gaussian noise, gray-scale change, contrast change, illumination and small 3D rotation) are added into the original optical images of four objects from COIL-100 database, as shown in Fig. 9. To show the different robustness between FIMA and AD-FIMA, two objects with parallelogram contour are chosen to test.

When the original image is disturbed by zero-mean white Gaussian noise of different variances (σ=0−0.05), the average feature diversities of the four algorithms are compared, as shown in Fig. 10. The average diversities of EC-ARC and GAO are above 0.2. FIMA and AD-FIMA show better stability and the average diversities are 0.16 and 0.18, respectively. Meanwhile, it is obvious that when the noise variance is below 0.02, the diversity of our proposed algorithms is quite small

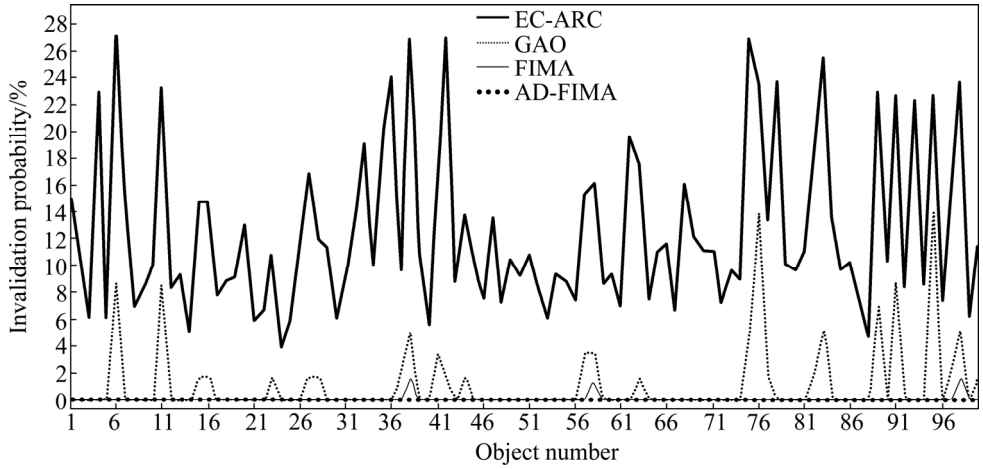

Fig. 7 Average invalidation probability of four algorithms when extracting affine invariant features of all images

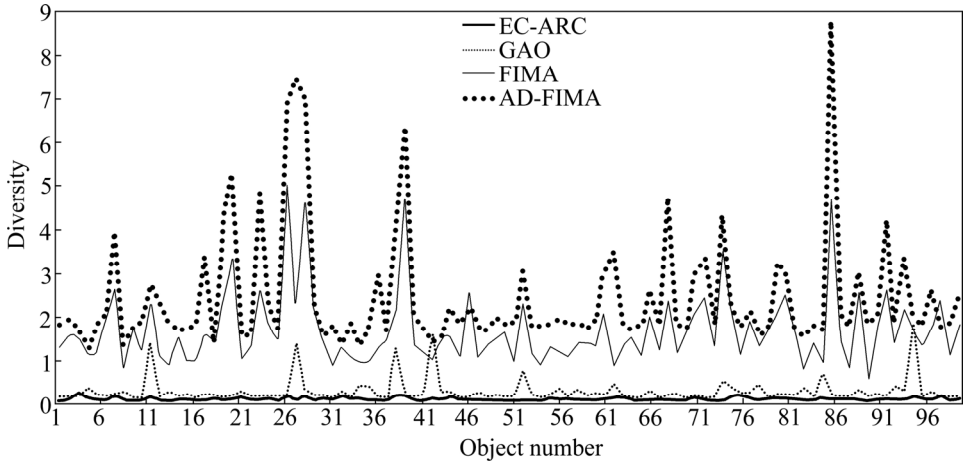

Fig. 8 Average feature diversity between every object and others when applying four algorithms

Fig. 9 Four objects chosen for robustness test

(≤0.05). It is proved that FIMA and AD-FIMA have better robustness for additive white Gaussian noise.

Figure 11 shows the average feature diversities of the four algorithms when the original image is disturbed by different gray-scale change (Δ*G*=5−30). It is shown that all the algorithms have more diversities with

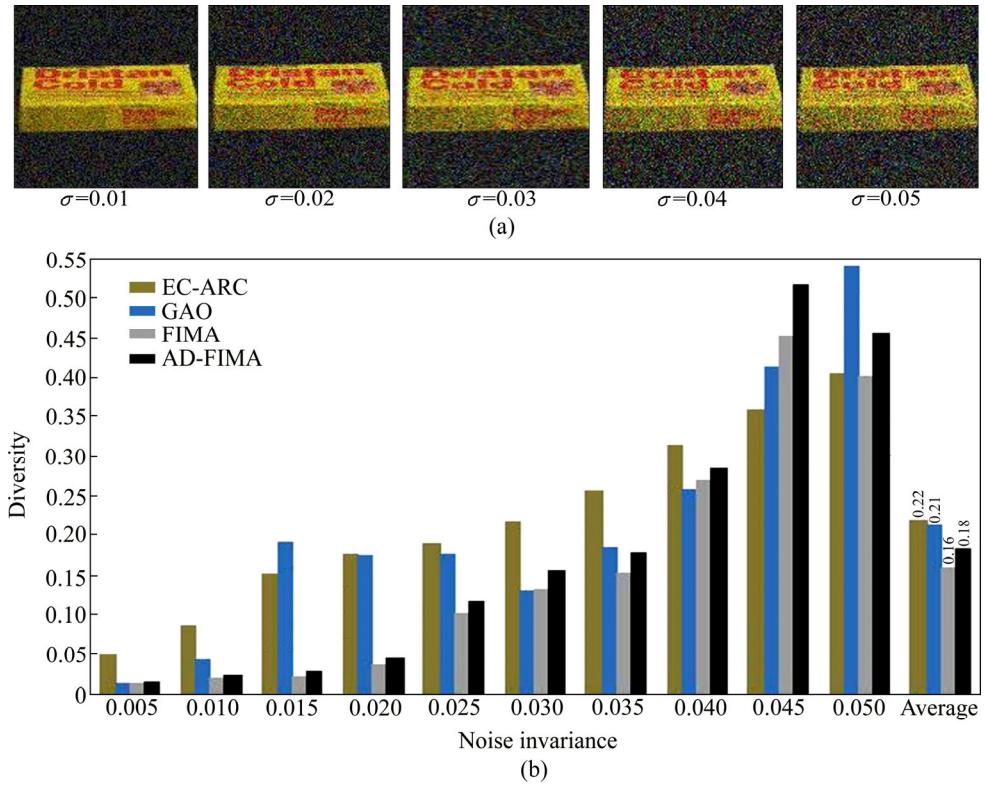

Fig. 10 Examples of images with Gaussian white noise (a) and average feature diversities of four algorithms with origin image disturbed by zero-mean Gaussian white noise of different variances (b)

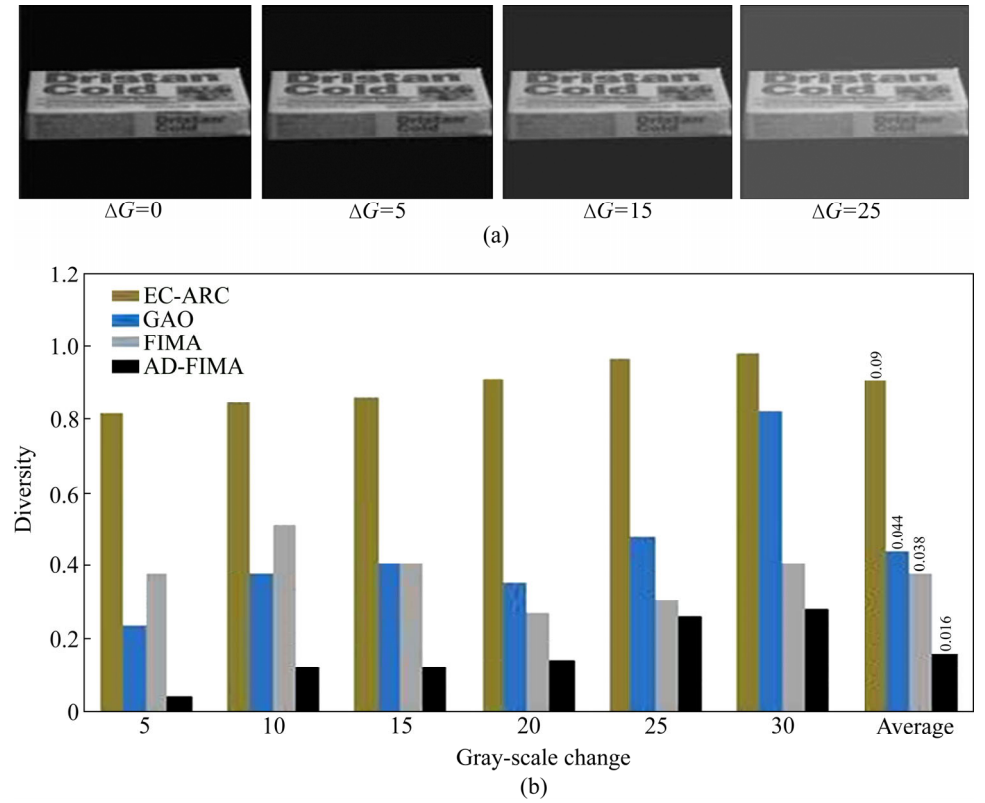

Fig. 11 Examples of images with gray-scale change (a) and average feature diversities of four algorithms with original image disturbed by different gray-scale changes (b)

increasing the gray-scale change. However, compared with EC-ARC and GAO, FIMA and AD-FIMA has much less diversities, and the average diversities are 0.038 and 0.016, respectively. Thus, our new algorithms show their better robustness for the gray-scale change, and they are preferred in practice.

Figure 12 depicts the comparison of the average feature diversities of the four algorithms when the original image is disturbed by different contrast change (ΔC=5−30). It is shown that all the four algorithms have good robustness for the change of contrast. Their average diversities maintain approximately at 0.005. Yet it is known that AD-FIMA has the best stability and the average is less than 0.003. Therefore, it is proved that the contrast change does not affect these algorithms much.

Different intensities (I=0−100 cd) of illumination are added to disturb the images, and the examples are shown in Fig. 13. It is found that the illumination affects the original image sharply, which even covers up many detailed local information and change many global

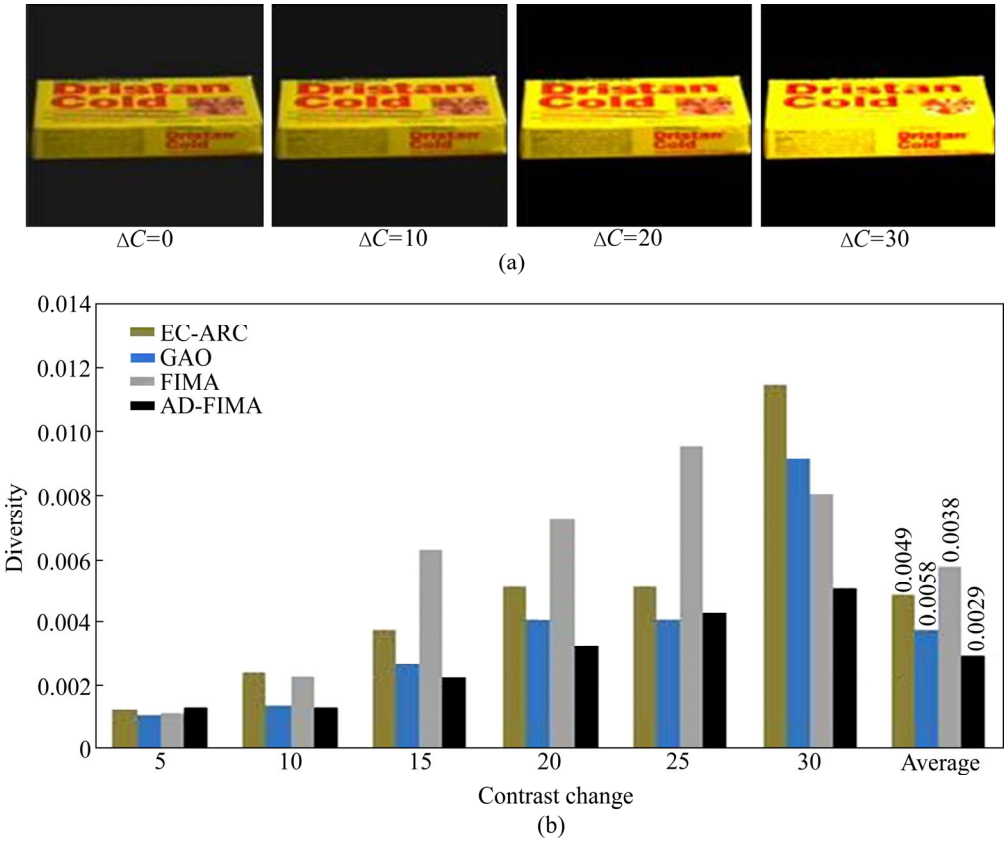

Fig. 12 Examples of images with contrast change (a) and average feature diversities of four algorithms with original image disturbed by different contrast changes (b)

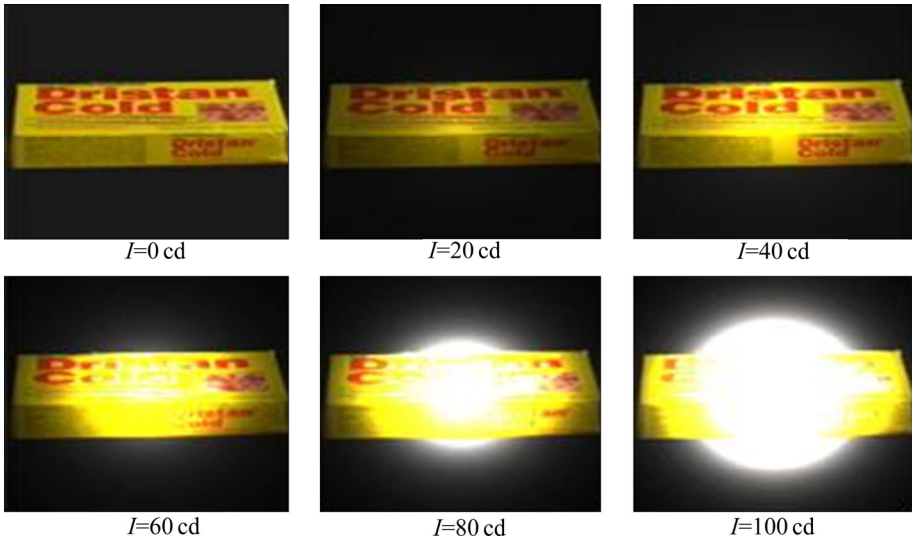

Fig. 13 Examples of images with different intensities of illumination

information such as the contour. Table 1 lists the average diversities of the four algorithms when the original image is disturbed by different intensities of illumination. It is expressed that the average diversities of all these algorithms are approximately 0.3.

Table 1 Average diversities of four algorithms with original image disturbed by different intensities of illumination

Illumination intensity	Average diversity			
	EC-ARC	GAO	FIMA	AD-FIMA
10	0.4045	0.1659	0.1019	0.0523
20	0.2860	0.2170	0.2331	0.2303
30	0.3772	0.1793	0.3442	0.3031
40	0.2240	0.2261	0.3415	0.2822
50	0.5620	0.3302	0.2988	0.3432
60	—*	0.2372	0.2179	0.4540
70	—	03062	0.8614	0.4945
80	—	—	0.5301	0.5303
90	—	—	0.5581	0.5820
100	—	—	—	0.5197
Average	0.309	0.207	0.348	0.345

Note: * means that invalidation problem happens during test.

However, compared with EC-ARC and GAO, the average diversity of different objects of FIMA and AD-FIMA is about 10 times higher than the effect of illumination, so target can be recognized even if the intensity of illumination is strong. Meanwhile, as the intensity of illumination increases, the invalidation problems happen in EC-ARC, GAO and FIMA. Thus, it is proved that AD-FIMA has the best robustness for the disturbance of illumination among the four algorithms.

Figure 14 shows the average feature diversities of the four algorithms when the original image is disturbed by 3D rotation from −30° to 30°. 3D rotation does not belong to affine transformation, thus the extracted affine features would change with 3D rotation. Yet when the rotation is small, the transformation is approximately affine. In Fig. 14, it is shown that when rotation is small (0°−15°), the diversities of FIMA and AD-FIMA are much lower. Hence, it is proved that FIMA and AD-FIMA have better robustness for small 3D rotation. However, all the four algorithms will be invalid with the increase of 3D rotation. In the actual work, in order to be robust for 3D rotation, two methods are utilized. Firstly, it is necessary to build more integrated pattern database of targets. Secondly, the iterative image matching algorithms [17−18] are quite available.

5.4 Computing performance

Table 2 gives the comparison of the time consumptions of the four algorithms when they process the images of different sizes. Comparison results demonstrate that FIMA and AD-FIMA have a speedup of approximate 1.75 times higher than EC-ARC and GAO. Because the function pow in math library is utilized to

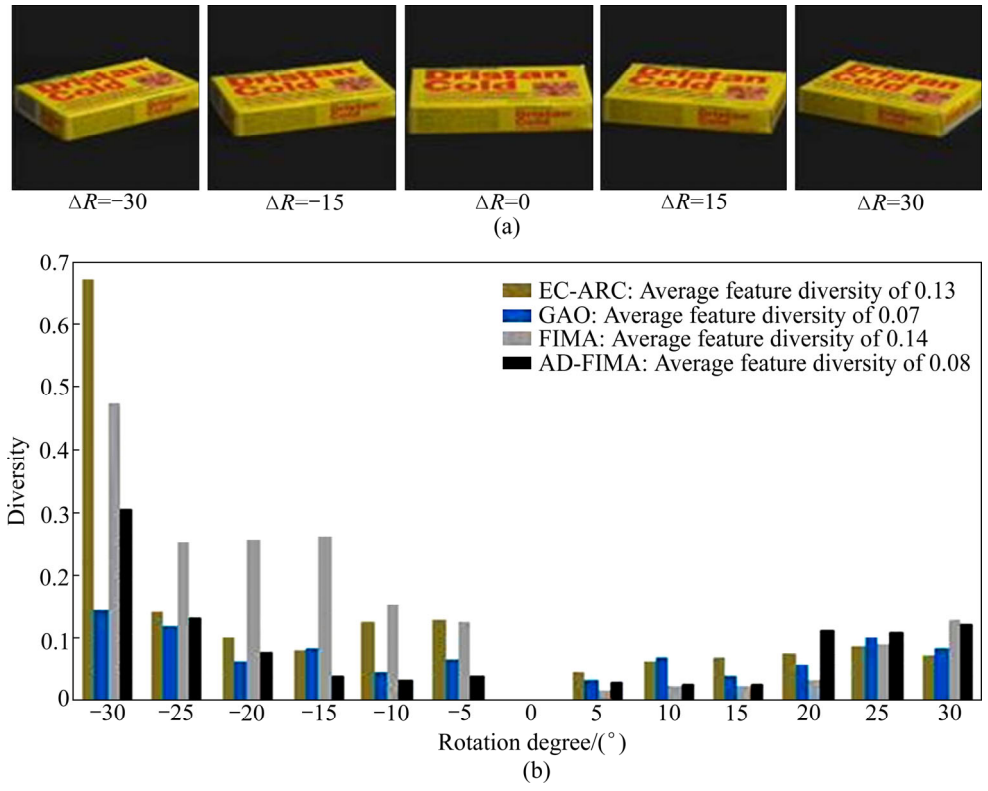

Fig. 14 Examples of images with 3D rotation (a) and average feature diversities of four algorithms with original image disturbed by 3D rotation from −30° to 30° (b)

Table 2 Comparison of time consumption of four algorithms when processing images of different sizes (ms)

Algorithm	128×128	256×256	384×384	512×512	640×640	768×768	896×896	1024×1024	Average
EC-ARC	6.1	15	39.22	73.12	119.69	176.47	237.82	312.19	122.451
GAO	6.09	15.15	37.96	72.81	119.53	175.62	237.66	310.9437	121.970
FIMA	4.84	8.75	22.97	42.65	69.53	102.34	138.75	180.47	71.288
AD-FIMA	5	8.2	21.34	40.84	66.69	101.56	137.22	177.35	69.775

calculate the EC, the time cost of extracting extended centroid is not in a linear relationship with its level. Thus, the actual speedup is different with the result of theoretical analysis in Section 4.2. However, this difference does not affect the qualitative analysis that FIMA and AD-FIMA have better performance. Meanwhile, for most images in COIL-100, the two-level EC does not coincide with centroid, and AD-FIMA could utilize it to build affine invariants, thus the speed of AD-FIMA is the highest in all the four algorithms.

However, when partial occlusion happens or multi targets are contained in a complex optical image, they would be invalid compared with the local feature-based algorithms. Hence, some novel hybrid algorithms [4, 19−20] motivate us to combine FIMA or AD-FIMA with some local feature-based algorithms for recognizing target better in the future work.

Because our new proposed algorithms utilize the contours of target to build line segments, it is apparently that precise contours extracting algorithm [21] is depended on FIMA and AD-FIMA compared with other algorithms. How to modify them to alleviate the dependence of contours extracting algorithms will also be concerned in the further research. Besides, quantum computation becomes hot topic. Utilizing quantum mechanics can achieve an amazing speedup for most image processing tasks. Hence, in the future work, we will also focus on how to design quantum image matching algorithms based on existing quantum image representations [22−23].

6 Conclusions

1) Based on global affine invariant feature of the length ratio of two parallel line segments, a fast image matching algorithm (FIMA) overcomes the zero-feature invalidation of the algorithms based on the area ratio of affine region. In order to address the parallelogram edge problems and the coincidence invalidation of FIMA, AD-FIMA is proposed to enhance FIMA.

2) FIMA and AD-FIMA increase the feature diversity of different targets and thus could be expected to reduce misjudgment rate during recognizing single target in optical images. Both of them have excellent robustness for additive white Gaussian noise, gray-scale change, contrast change, illumination and small 3D rotation. Compared with the fast latest algorithms based on geometry feature, FIMA and AD-FIMA can reach the speedup of approximately 1.75 times. Therefore, FIMA and AD-FIMA would be very significant and suitable for actual ATR applications.

3) FIMA and AD-FIMA belong to the global feature-based algorithms, and they have better performance and robustness than any other state-of-the-art algorithms based on global geometry feature.

References

[1] ZITOVA B, FLUSSER J. Image registration methods: A survey [J]. Image and Vision Computing, 2003, 21(11): 977−1000.

[2] HU M K. Visual pattern recognition by moment invariants [J]. IRE Transactions on Information Theory, 1962, 8(2): 179−187.

[3] LEI Lin, CHEN Tao, LI Zhi-yong, SU Yi. A New approach to image invariant extraction under global affine transformation [J]. Journal of National University of Defense Technology, 2008, 4: 64−70. (in Chinese)

[4] LISIN D A, MATTAR M A, BLASCHKO M B. Combining local and global image features for object class recognition [C]// IEEE Computer Society Conference on Computer Vision and Pattern Recognition-Workshops. Washington DC: IEEE, 2005: 47−47.

[5] LOWE D G. Distinctive image features from scale-invariant keypoints [J]. International Journal of Computer Vision, 2004, 60(2): 91−110.

[6] BAY H, TUYTELAARS T, GOOL L. Surf: Speeded up robust features [M]. Computer Vision–ECCV 2006. Graz, Austria: Springer Berlin Heidelberg, 2006: 404−417.

[7] MATAS J, CHUM O, MARTIN U, PAJDLA T. Robust wide baseline stereo from maximally stable external regions [J]. Image and Vision Computing, 2004, 22(10): 761−767.

[8] AMIRI M, RABIEE H R. RASIM: A novel rotation and scale invariant matching of local image interest points [J]. IEEE Transactions on Image Processing, 2011, 20(12): 3580−3591.

[9] RAHTU E, SALO M, HEIKKILA J. Affine invariant pattern recognition using multi scale auto convolution [J]. IEEE Transactions on PAMI, 2005, 27(6): 908−918.

[10] CHEN Tao, SU Yi, JIANG Yong-mei, TANG Tao, YU Wen-xian. Affine invariant feature extraction based on affine geometry [J]. Journal of Image and Graphics, 2007, 12(9): 1633−1641. (in Chinese)

[11] GAO Feng, WEN Gong-jian. A new method for affine invariants extraction based on affine geometry [J]. Journal of Image and Graphics, 2011, 16(3): 389−397. (in Chinese)

[12] CHRISTO D, PRINCE J L, BRYAN R N. Image registration based on boundary mapping [J]. IEEE Transactions on Medical Imaging, 1996, 15(1): 112−115.

[13] YANG Z, COHEN F S. Image registration and object recognition using affine invariants and convex hulls [J]. IEEE Transactions on Image Processing, 1999, 8(7): 934−946.

[14] BIAN Xing-bin, ZHU Qing-xin. Analysis of moment invariants stability to gray-level adjustment [C]// Proceedings of ICSSM'05. Washington DC, USA: IEEE Computer Society, 2005: 1145−1148.

[15] NENE S A, NAYAR S K, MURASE H. Columbia object image library (COIL-100) [R]. Technical Report CUCS-005-96. New York: Columbia University, 1996.

[16] QU Zhi-guo, WANG Ping, GAO Ying-hui. Randomized SUSAN edge detector [J]. Optical Engineering, 2011, 50(11): 110502−110502-3.

[17] YU Yi-nan, HUANG Kai-qi, CHEN Wei, TAN Tie-niu. A novel algorithm for view and illumination invariant image matching [J]. IEEE Transactions on Image Processing, 2012, 21(1): 229−240.

[18] MOREL J M, YU G. ASIFT: A new framework for fully affine invariant image comparison [J]. SIAM J Imag Sci, 2009, 2(2): 438−469.

[19] HARDER M, POLANI D, NEHANIV C L. Think globally, sense locally: From local information to global features [C]// 2011 IEEE Symposium on Artificial Life. Paris: IEEE, 2011: 70−77.

[20] KURUZ B J. Optimal color quantization for color displays [C]// IEEE Conference on Computer Vision and Pattern Recognition. Washington DC, USA, 1983: 217−224.

[21] XIANG Zhi-gan. Color image quantization by minimizing the maximum intercluster distance [J]. ACM Transactions on Graphics, 1997, 16(3): 260−276.

[22] ZHANG Yi, LU Kai, GAO Ying-hui, WANG Mo. NEQR: A novel enhanced quantum representation of digital images [J]. Quantum Information Processing. 2013, 12(8): 2833−2860.

[23] ZHANG Yi, LU Kai, GAO Ying-hui, XU Kai. A novel quantum representation for log-polar images [J]. Quantum Information Processing. 2013, 12(9): 3103−3126.

(Edited by FANG Jing-hua)